

A SYNERGISTIC ABSORPTION AND PLASMONIC EFFECT OF SiO₂@Au@TiO₂ IN A TiO₂ PHOTOANODE FOR DYE-SENSITIZED SOLAR CELLS

M. N. Pakpahan, A. Hartanto, Y.D. Gultom, N. Fadhilah and D.D. Risanti

Department of Engineering Physics, Faculty of Industrial Technology and Engineering System, Institut Teknologi Sepuluh Nopember Surabaya, Kampus ITS Keputih Sukolilo, Surabaya 60111, Indonesia

E-mail: risanti@ep.its.ac.id

Received: 6 January 2021

Revised: 12 April 2021

Accepted: 20 April 2021

ABSTRACT

A SYNERGISTIC ABSORPTION AND PLASMONIC EFFECT OF SiO₂@Au@TiO₂ IN A TiO₂ PHOTOANODE FOR DYE-SENSITIZED SOLAR CELLS. A method for increasing the visible-light harvesting of a TiO₂ anatase photoanode in dye-sensitized solar cells by incorporating plasmonic nanostructures was developed. Sidoarjo mud as the SiO₂ source was used to successfully synthesized core/multishell SiO₂@Au@TiO₂, with varying amounts of Au (60, 90, and 120 mL). In addition, the core/multishell fractions in TiO₂ paste were varied, i.e., 0.5%, 1%, and 5%. The UV-Vis spectrum shows that a more ripple spectrum at higher wavelengths is obtained with increasing Au content, as suggested by the presence of large Au nanoparticles; however, a similar value of efficiency is observed for all sample variations studied compared to a pure TiO₂ photoanode. The incident photon-to-current efficiency reveals that all photoanodes containing the core/multishell SiO₂@Au@TiO₂ studied show somewhat broader and enhanced spectra for all studied wavelengths compared to the pure TiO₂ photoanode, resulting from the synergistic effect between plasmonic nanostructures and the presence of silica that boost the absorption to higher wavelengths.

Keywords: Dye-Sensitized Solar cells, Plasmonics, Absorption, Silica

ABSTRAK

PENYERAPAN SINERGI DAN EFEK PLASMONIK SiO₂@Au@TiO₂ DALAM FOTOANODE UNTUK SEL SURYA TERSENSITISASI PEWARNA. Untuk meningkatkan pemanenan cahaya tampak di dalam *Dye-Sensitized Solar Cells* (DSSC), anoda foto TiO₂ ditambahkan dengan struktur nano plasmonik. Struktur nano *core/multishell* SiO₂@Au@TiO₂ dengan SiO₂ yang digunakan berasal dari hasil ekstraksi lumpur Sidoarjo telah disintesis dan dicampurkan ke dalam anoda foto TiO₂. Di samping itu, jumlah Au dalam struktur *core/multishell* yang divariasikan dengan jumlah 60 ml, 90 ml, dan 120 ml. Fraksi *core/multishell* SiO₂@Au@TiO₂ terhadap pasta TiO₂ divariasikan, yakni 0,5%, 1%, dan 5%. Dari hasil pengujian UV-Vis terlihat bahwa absorpsi dari SiO₂@Au@TiO₂ hanya berbeda pada panjang gelombang yang besar sebagai efek dari adanya kluster partikel nano dalam ukuran besar, namun demikian nilai efisiensi dari ketiga variasi Au dengan 3 variasi fraksi tidak menunjukkan hasil yang signifikan dibandingkan dengan anoda foto dengan TiO₂ saja. Hasil uji *Incident Photon-to-Current Efficiency* (IPCE) menunjukkan hal serupa seperti kurva J-V, spektrum dari anoda foto dengan struktur *core/multishell* SiO₂@Au@TiO₂ sedikit lebih tinggi dan lebar dibandingkan dengan anoda foto TiO₂ saja. Hal ini menunjukkan efek sinergistik dari plasmonik dan keberadaan silika di dalam struktur nano tersebut.

Kata kunci: Dye-Sensitized Solar Cells, Plasmonik, Absorpsi, Silika

INTRODUCTION

Enhanced light absorption in dye-sensitized solar cells (DSSCs) with high performance is of paramount importance [1]. Nanosized semiconductors with properties such as a high surface-to-volume ratio compared with bulk materials have been used as the mesoporous layer in DSSCs, which is known to boost the light absorption potential of these solar cells [2]. However, nanomaterials with a size of less than H^*50 nm, such as those used in the mesoporous layer of the DSSCs, cannot adequately either scatter or reflect sunlight [3]. Efforts have been concentrated on synthesizing materials based on SiO_2 as a scattering material either in the form of a core/shell [4] or as a microsheat [5] and SiO_2 extracted from Sidoarjo mud that can scatter the incoming light as these materials are incorporated into the mesoporous layer, such as simple core/shell materials [6,7], core/multishell materials [8–10], and silica microsheat [11,12]. These light-scattering materials usually have a low surface area, and thus, they can reduce light harvesting in the light-sensitized coating of the mesoporous layer. Therefore, one needs to tailor scattering materials without deteriorating their ability to absorb light. Among the abovementioned materials, we focused on core/multishell particles.

A method of using gold- or silver-based plasmonic metal nanoparticles is often used for improving photoanode solar cell systems. A prevailing evanescent electromagnetic wave on the surface of these nanostructures is produced when the electric field of light encounters the free electron in the Au or Ag nanostructures. Collective electron oscillations on the surface of the nanoparticle induce a phenomenon called local surface plasmon resonance (LSPR) at a particular wavelength of light that brings about intense light extinction (absorption and scattering). These relative merits have been employed as an enhancement element in the photoanode of DSSCs [13–15] and quantum dot [16].

Kim et al. reported core/multishell structure $SiO_2@TiO_2@Au$ showing an increment in short-circuit current leading to a marked rise in efficiency by 14% [17]. Likewise, it was shown that core/multishell $SiO_2@TiO_2@Au$ using SiO_2 extracted from Sidoarjo mud can increase the short-circuit current [9], thus raising the efficiency 1.9 times higher than the pure TiO_2 photoanode. Meanwhile, core/multishell $TiO_2@SiO_2@Au$ did not show improvement in short-circuit current, which is attributed to the difficulty of the

electron to transfer from Au to TiO_2 . On the other hand, a previous study reported that the Au core surrounded by SiO_2 and TiO_2 can boost efficiency to 5.52% [18], better than pure TiO_2 only. However, the efficiency obtained was small [10]. Other studies incorporating the core/multishell $SiO_2@Au@TiO_2$ with SiO_2 synthesized from tetraethyl orthosilicate indicated the positive contribution of the multishell particles in the TiO_2 photoanode in increasing the efficiency to almost twice, compared to solely the TiO_2 photoanode [19–21].

The $SiO_2@Au@TiO_2$ structure as stated in other studies [19, 20] provides the extension of light travels within the photoanode due to the intense light scattering effect, a highly favored light absorption leading to a remarkable photogenerated carrier production through the dispersion of Au nanoparticles. Finally, the outer layer of TiO_2 is auspicious for localization of incident light that encourages the dye to deliver more charge carriers, and the Schottky barrier established at the Au– TiO_2 interface accelerates electron transfer to the external circuit.

The main aims of the study were to investigate the effects and mechanisms of the Au volume fraction in the $SiO_2@Au@TiO_2$ core/multishell and the fraction of the $SiO_2@Au@TiO_2$ core/multishell in the photoanode on its optical properties and to explore its impact on the performance of DSSCs. Herein, the electromagnetic scattering of Au nanoparticles in the core/multishell was studied using the boundary element method. The results were compared to the photoconversion ability of the studied DSSCs.

EXPERIMENTAL METHOD

Materials and Instruments

Sidoarjo mud, 37% HCl, NaOH, 28% NH_4OH , ethanol (EtOH), Aquadest, acetic acid (98%, CH_3COOH), potassium iodide (KI), iodide (I), PEG 4000, and ammonium (25% NH_3) were used. $TiCl_3$, trisodium citrate ($C_6H_5Na_3O_7 \cdot 2H_2O$), chloroform, and Triton X-100 were supplied by Merck. (3-Aminopropyl) trimethoxysilane (APTMS, 97%), $HAuCl_4 \cdot 3H_2O$ (49%), titanium(IV) isopropoxide (TTIP, 97%), triethanolamine (TEOA, 99%), and mercaptoundecanoic acid (MUA, 95%) were procured from Sigma Aldrich. Acetonitrile was supplied by Fulltime Chemical Corp. Ruthenium N-719 was purchased from Dyesol. Deionized water was used in all experiments. 3.2 mm-thick ($8 \Omega/sq$) fluorine-doped tin oxide (FTO) glass 20 mm \times 20 mm in size and Pt-coated

FTO glass as the counter electrode with the same dimensions for assembly of DSSC were purchased from Dyesol.

X-Ray Diffractometer (XRD, Philips X'Pert MPD) was performed on the nanoparticles obtained from mud extraction and core/shell synthesis with Cu-K α radiation ($\lambda = 1.5405 \text{ \AA}$). SEM images were recorded using an FEI S-50 at the Department of Materials and Metallurgy ITS, a JEOL JIB-4610F at the Research Center for Physics, Indonesian Institute of Sciences, and a Hitachi SU3500 at the Research Center for Nanoscience and Nanotechnology (RCNN) ITB. Transmission Electron Microscopy (TEM) was performed on an FEI Tecnai G2 20 S-Twin operated at 200 kV. The absorption spectra of the core/multishell SiO₂@Au@TiO₂ were measured using a UV-Vis Lambda 750 spectrophotometer in the visible-light range of 380 to 700 nm. Current and voltage measurements were carried out using a solar simulator that used a halogen lamp as the source and was connected *via* a PXI-E1073 and SMU PXI-4130. Incident Photon-to-Current Efficiency (IPCE) measurements were done involving a monochromator (CT-10T, JASCO) and halogen lamp (GR-150), with a distance between them of 4 cm. The distance between the DSSC and the monochromator was 1 cm. The power at each wavelength of the halogen lamp was measured using a Power Meter (Thorlab S-120C).

Plasmonic excitation of the Au NP surrounded by a dielectric environment in response to the incident visible-light was studied using a free MNPBEM toolbox for MATLAB, which employs the boundary element method approach [22], presents a solution to Maxwell's equations for a dielectric system, and allows for the consideration of a layered environment that is suitable for core/shell or core/multishell systems.

Method and Procedure

Extraction of SiO₂ nanoparticles from Sidoarjo mud, synthesis of the TiO₂ photoanode, and Au nanoparticle reduction were performed by the reported method [8,9]. First, the obtained Sidoarjo mud was dried, ground, and sieved through a 250 mesh screen to a fine powder. The powder was soaked overnight in 2 M HCl, then washed with distilled water, dried, ground again to remove the agglomerated powder, and sieved through a 25 mesh screen. Ten grams of the powder was dissolved in 60 mL of 7 M NaOH solution with vigorous stirring for 1 h at 70 °C. About 250 mL of distilled water was added dropwise to the solution, and the solution was cooled

to room temperature. The solid product was collected by filtration and then titrated with 2 M HCl to neutralize the pH until a white precipitate was obtained. The SiO₂ suspension was kept at room temperature for 24 h to let gravity separation occur, and the product was subsequently filtered and washed with distilled water until there was a negative reaction for chlorine ions. The final SiO₂ product with a particle size of about 52–65 nm was eventually dried at 80 °C for 24 h.

The reduction of Au required six times processes to obtain a total of 270 mL of Au solution, which was then divided into 60, 90, and 120 mL. The Turkevich method was used to reduce Au from HAuCl₄·3H₂O. First, to an Erlenmeyer tube, 2.5 mL of HAuCl₄·3H₂O was mixed with 50 mL of deionized water and boiled at 150 °C. Afterward, 2 mL of trisodium citrate as the reducing agent was added under vigorous stirring with a magnetic stirrer. After 7 min, the color of the mixture changed from white, to purple, to red purple. Cooling to room temperature turned the color into dark red, indicating the successful synthesis of Au nanoparticles.

The SiO₂@Au core/shell structure was synthesized as follows. First, the SiO₂ solution was prepared by dissolving 0.5 g of powdered SiO₂ nanoparticles from Sidoarjo mud in a solvent mixture containing 0.7 mL of distilled water, 2 mL of ammonia, and 39.5 mL of ethanol. This mixture was stirred for 1 h to obtain a homogeneous SiO₂ solution. This solution was eventually modified with 0.4 mL of APTMS and subsequently mixed with the second solution, i.e., Au solution. To produce a SiO₂@Au@TiO₂ core/shell, the SiO₂@Au solution was treated with 0.4 μ L of MUA, then kept for 2 h, and eventually added with 30 mL of TiO₂ solution. The TiO₂ shell was obtained from the process of mixing TTIP with TEOA under a nitrogen atmosphere at a molar ratio of TEOA/TTIP = 2:1. TEOA was added to the Ti⁴⁺ stock solution at room temperature. Afterward, water was added to prepare 0.50 M Ti⁴⁺ solution. The SiO₂@Au@TiO₂ core/shell solution was further titrated to pH 7 under continuous stirring until a white precipitate was formed. The precipitate was filtered, then washed with distilled water to remove any remnants of acid, alkaline, and salt. Finally, the precipitate was dried at 80 °C for 24 h, and the core/multishell powder was obtained.

This research used an anatase TiO₂ and core/multishell fraction of 0.5% and 1%, respectively. For each volume fraction, the amount of SiO₂ core in the core/multishell SiO₂@Au@TiO₂ nanoparticles was varied from

60 to 120 mL. For paste preparation, 0.25 g of nanoparticle powdered photoanode material was then dissolved in a mixed solvent of 87.5 μL of distilled water, 125 μL of CH_3COOH , and 12.5 μL of Triton X-100. The paste was coated on FTO glass using the doctor blade method onto the active area of the photoanode having a size of 0.5 cm \times 0.5 cm. The coated paste was immediately heated at 225 $^\circ\text{C}$ for 2 min using a hot plate.

RESULTS AND DISCUSSION

The XRD spectra of the synthesized $\text{SiO}_2@\text{Au}@\text{TiO}_2$ shown in Figure 1 show the Au (JCPDS No. 00-004-0784), SiO_2 (JCPDS No. 00-005-0490), and TiO_2 (JCPDS No. 21-1272) peaks, demonstrating their co-existence in the obtained structure.

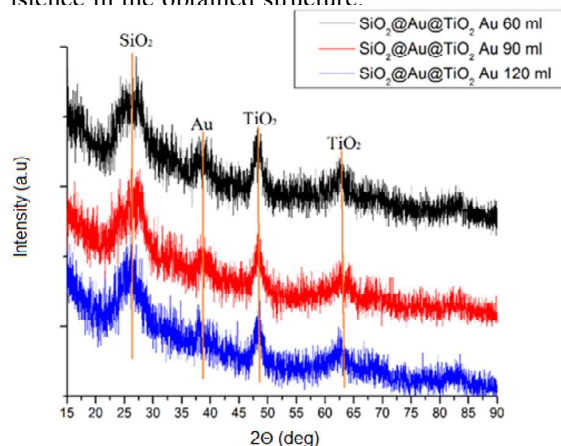


Figure 1. XRD spectra of core/multishell $\text{SiO}_2@\text{Au}@\text{TiO}_2$ with different contents of Au.

Figure 2 exhibits the morphologies for each step of the synthesis process of $\text{SiO}_2@\text{Au}@\text{TiO}_2$. SiO_2 extracted from the mud is irregular and polydispersed with sizes of 51–65 nm (Figure 2(a)). The morphology of $\text{SiO}_2@\text{Au}$ is similar to that of SiO_2 (Figure 2(b)), but the structures tend to agglomerate in sizes of about 5 μm , measured by the line measurement tool of ImageJ software. The SEM image $\text{SiO}_2@\text{Au}@\text{TiO}_2$ (Figure 2(c)) shows a reduction in size, to about 1 μm .

The TEM images in Figure 3 of $\text{SiO}_2@\text{Au}@\text{TiO}_2$ with 90 mL of Au show the Au nanoparticle (black particle) in the agglomerated form and its uneven distribution, with an estimated size of ~ 25 nm, as measured by ImageJ.

Light absorption is a notable characteristic of an increased performance of solar cells. The normalized UV–Vis spectrum (Figure 4) reveals a continuous decrease toward a higher wavelength without any remarkable peak around the Au plasmon resonance region, indicating that

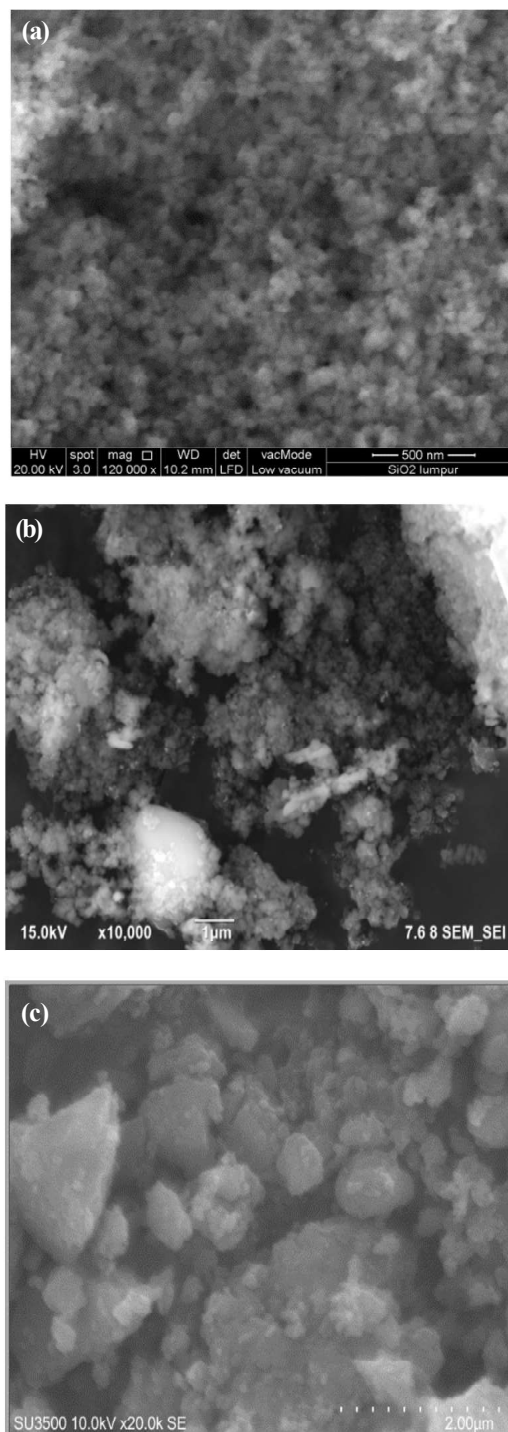


Figure 2. SEM images of (a) SiO_2 extracted from Sidoarjo mud, (b) $\text{SiO}_2@\text{Au}$, and (c) $\text{SiO}_2@\text{Au}@\text{TiO}_2$.

Au is attached to SiO_2 . In addition, a more ripple spectrum at higher wavelengths is obtained with increasing Au content, leading to a stronger absorbance. The difference stems from different surface coverages of Au for the same APTMS amounts. A study [23] revealed enhanced absorption for agglomerated Au nanoparticles on SiO_2 , particularly around the plasmon resonance region due to the collective effect of plasmon–plasmon interactions

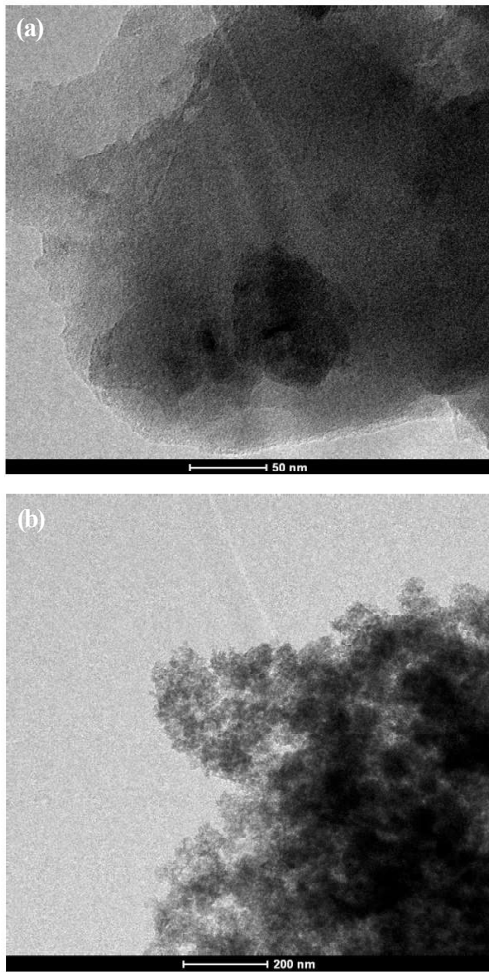


Figure 3. TEM images of SiO₂@Au@TiO₂: (a) close examination of a single core/multishell and (b) overview examination.

but a SiO₂-dominated extinction spectrum for singly or less attached Au nanoparticles on SiO₂.

Results for the MNPBEM simulation extinction cross sections on the SiO₂@Au and SiO₂@Au@TiO₂ structures are shown in Figure 5. At higher wavelength, the multishell SiO₂@Au@TiO₂ shows a remarkable peak, attributed to the resonance wavelength of the particle, as compared to SiO₂@Au. The extinction calculated through MNPBEM is the sum of scattering and absorption [22].

Plasmonic coupling and aggregation among the particles determine shifting to higher wavelengths. It is known that when the size of the Au nanoparticles is >50 nm, the energy of oscillating electrons in the particles decreases due to the radiative damping effect and phase retardation of the charges, resulting in the increase in resonance wavelength and a decrease in the frequency of oscillating electrons [24].

As the nanoparticles are distributed in the form of clusters, they increase the near field leading to a larger

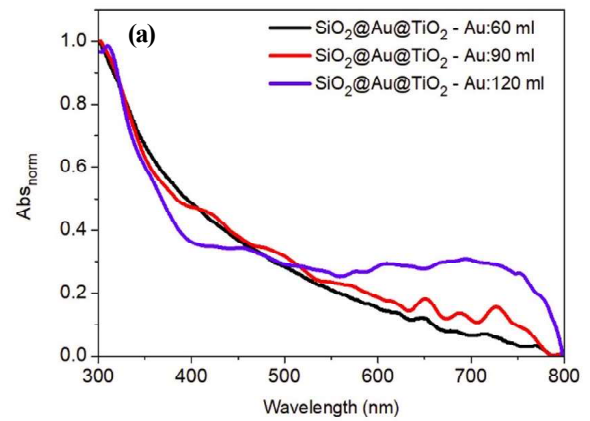


Figure 4. UV-Vis spectra of core/multishell SiO₂@Au@TiO₂ with different amounts of Au.

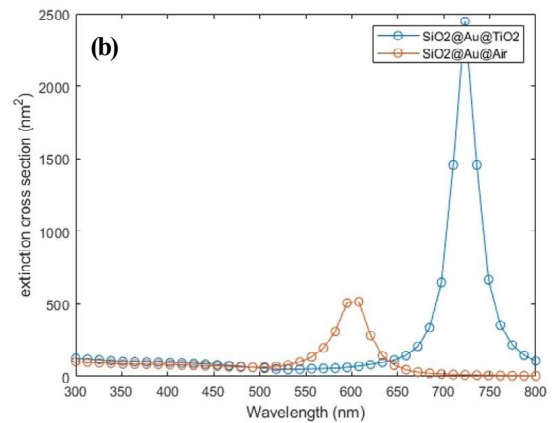


Figure 5. Extinction cross sections of single core/multishell SiO₂@Au and SiO₂@Au@TiO₂.

extinction cross section (Figure 6), in agreement with the literature [25]. It is seen in Figure 5(a) that a small cluster size of 10 nm reveals a very weak extinction cross section with a weak peak that appears at about 620 nm. A larger cluster size amplifies the extinction cross section. In this case, the core/multishell was simplified by using only Au nanoparticles dispersed in the form of clusters with specific interparticle spacing. A single particle contributes to the splitting of the extinction spectrum into several peaks with the intensity being reduced toward more isometric and compact topologies. On the other hand, the larger size of the particles leads to lower extinction spectra due to the reduction in dipolar excitation strength [26]. Thus, the sluggish ripple located at wavelengths above 600 nm in Figure 4 can be related to the presence of large particles of the core/multishell.

Table 1 shows the photovoltaic data of the DSSC studied, while Figures 7(c) show the *J-V* curves of cells fabricated with different concentrations of core/multishell structures with various Au contents and also of pristine DSSC without any core/multishell. It is seen

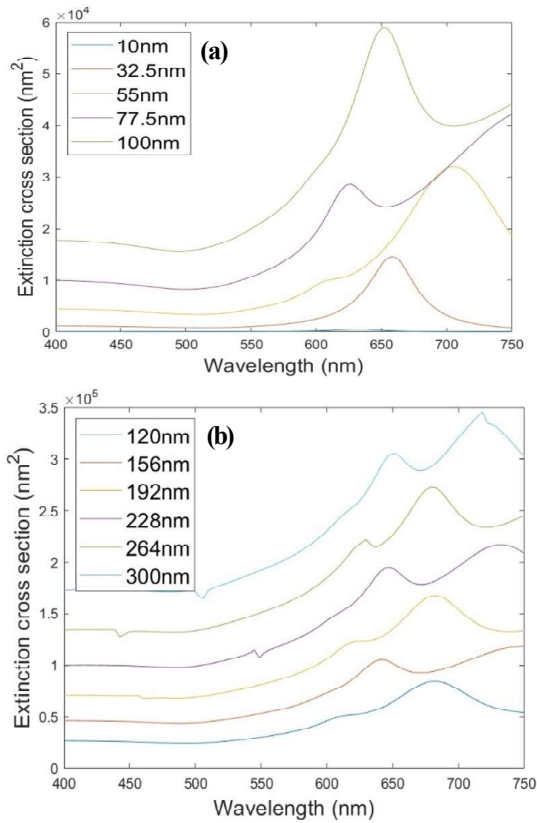


Figure 6. Extinction cross section of coupled Au particles embedded in TiO₂. The sizes of Au particles are indicated in the figure: (a) below 100 nm and (b) above 100 nm.

that the efficiency (η) generally falls within a similar value, which indicates that the presence of such a core/multishell does not improve the cell efficiency. Fill factors of the cells with core/multishell particles also do not change more significantly than that of the reference cell, exhibiting that the addition of the core/multishell, although the particles contain SiO₂, does not perturb the carrier transport through the sensitized layer [27].

It is noted that the presence of Au in the TiO₂ photoanode may slow down the recombination process by forming a Schottky barrier at the interface and acting

Table 1. The photovoltaic parameters of the dye-sensitized solar cells (DSSCs) based on the SiO₂@Au@TiO₂ core/multishell addition, with different Au quantities.

Name of Sample	J _{sc} (mA/cm ²)	V _{oc} (V)	FF	η (%)
Pristine TiO ₂	0.092	0.670	0.483	0.030
Au60-0.5%	0.110	0.710	0.490	0.038
Au60-1%	0.086	0.766	0.521	0.034
Au60-5%	0.076	0.687	0.506	0.026
Au90-0.5%	0.094	0.640	0.507	0.031
Au90-1%	0.083	0.679	0.520	0.029
Au90-5%	0.092	0.726	0.482	0.032
Au120-0.5	0.078	0.739	0.512	0.030
Au120-1%	0.079	0.808	0.505	0.032
Au120-5%	0.077	0.783	0.479	0.029

as an electron sink; however, its amount should be adjusted: 2.5% Au in the photoanode reported the lowest recombination [28], whereas more or even less Au contents may further lead to an increase in the recombination rate. On the other hand, agglomeration and uneven dispersion of Au nanoparticles as seen in Figure 3 cause more electron accumulation to allow the upward shift of the Fermi level [29]. However, these accumulated electrons cannot be further transferred to the conduction band of TiO₂, resulting in a poor photocurrent compared to pristine TiO₂.

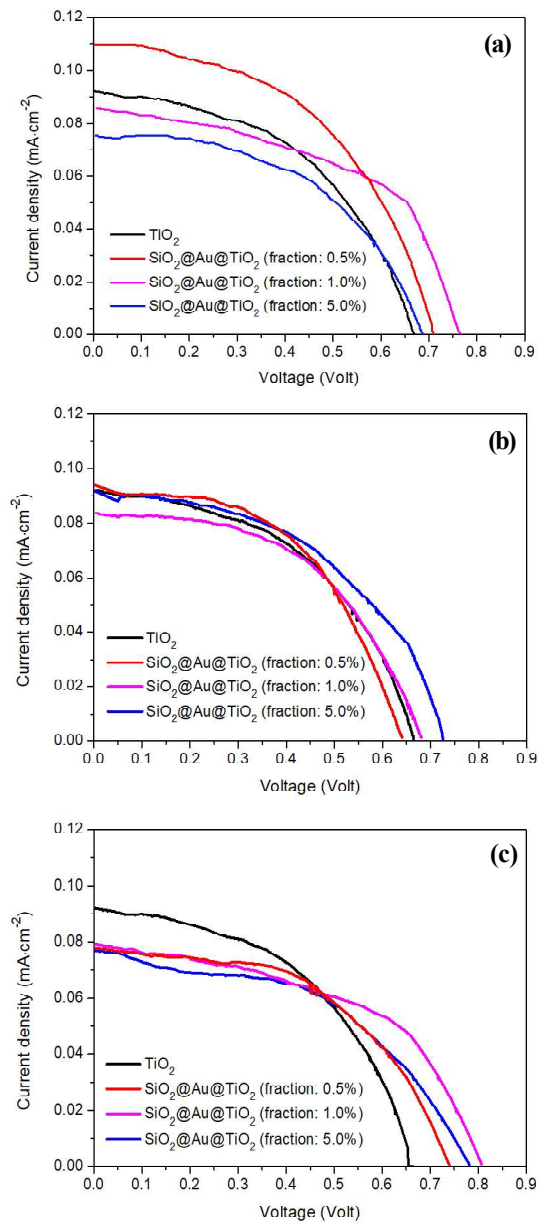


Figure 7. Dependence of photocurrent densities and conversion efficiencies of DSSCs comprising the TiO₂ photoanode in different proportions of the SiO₂@Au@TiO₂ core/multishell for (a) 60 mL of Au, (b) 90 mL of Au, and (c) 120 mL of Au in the core/multishell.

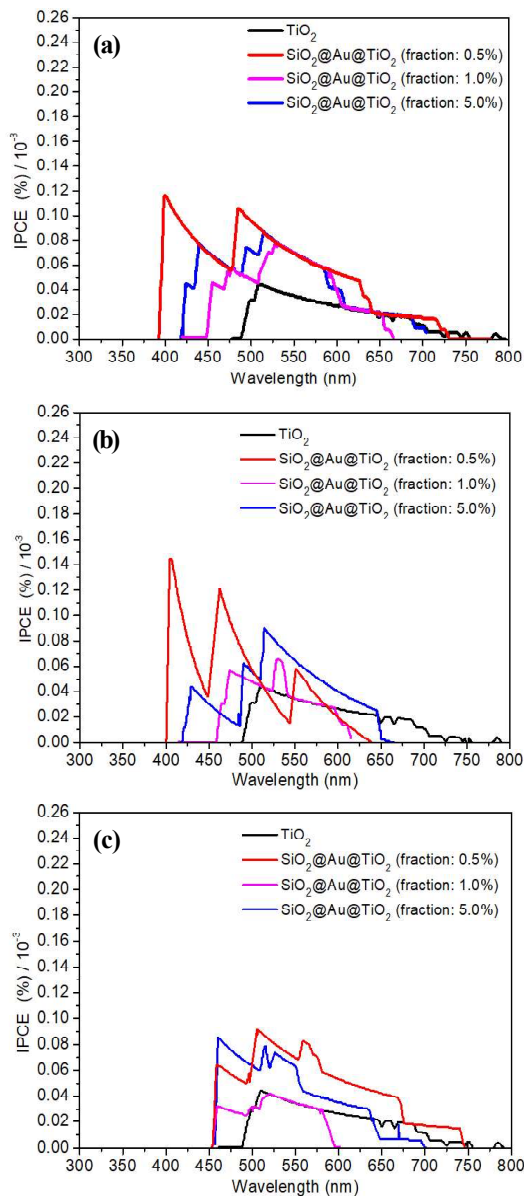


Figure 8. IPCE curves of the studied DSSCs for (a) 60 mL of Au, (b) 90 mL of Au, and (c) 120 mL of Au in the core/multishell.

The low J_{sc} obtained is well described to its IPCE as seen in Figure 8. Although the $J-V$ curves for all studied samples do not change significantly, the IPCEs of all samples shows a similar manner to the $J-V$ curves (Figure 7). The IPCE augmentation is detected over a wide spectral range rather than around the LSPR band of plasmonic nanostructures. The augmentation at the lower and mid-wavelength regions can be interpreted by two mechanisms: (i) the near-field effect of Au nanoparticles leading to increased dye excitation and (ii) contribution of the transfer of plasmon-induced excited hot electrons to the conduction band of TiO₂ [17]. Meanwhile, the enhancement taking place in the

longer wavelengths ($\lambda > 700$ nm) is the manifestation of the presence of silica particles.

CONCLUSION

The SiO₂@Au@TiO₂ core/multishell with Au contents varying from 60 to 120 mL was synthesized using Sidoarjo mud-extracted SiO₂. Although the absorbance of 60 mL of Au is the highest, the DSSC performance of studied samples is indistinguishable. However, the IPCE indicates that 90 mL of Au shows a remarkable broad and enhanced absorption for all studied wavelengths, which is due to the synergistic effect between plasmonic nanostructures and the presence of silica that boost the absorption to higher wavelengths. The fraction of the core/multishell embedded in TiO₂ should be kept as low as 0.5%.

ACKNOWLEDGEMENT

The authors would like to thank the Department of Engineering Physics Faculty of Industrial Technology and Engineering System Institut Teknologi Sepuluh Nopember Surabaya for funding this research under contract number: 1642/PKS/ITS/2020 and Dr.rer.nat. Ruri Agung Wahyuono for his help and fruitful discussion.

REFERENCES

- [1]. S. H. Hwang, D. H. Shin, J. Yun, C. Kim, M. Choi, and J. Jang. "SiO₂/TiO₂ hollow nanoparticles decorated with ag nanoparticles: enhanced visible light absorption and improved light scattering in dye-sensitized solar cells." *Chemistry – A European Journal*, vol. 20, no. 15, pp.4439–4446, Apr. 2014.
- [2]. S. H. Hwang, C. Kim, H. Song, S. Son, and J. Jang. "Designed architecture of multiscale porous TiO₂ nanofibers for dye-sensitized solar cells photoanode" *ACS Applied Materials & Interfaces*, vol. 4, no. 10, pp.5287–5292, 2012.
- [3]. M. Lickleder, R. Mohammadi, N. T. Nguyen, H. Park, S. Hejazi, M. Halik, N. Vogel, M. Altomare, and P. Schmuki. "Dewetted Au nanoparticles on TiO₂ surfaces: evidence of a size-independent plasmonic photoelectrochemical response?" *The Journal of Physical Chemistry C*, vol. 123, no. 27, pp.16934–16942, Jul. 2019.
- [4]. S. Son, S. H. Hwang, C. Kim, J. Y. Yun, and J. Jang. "Designed synthesis of SiO₂/TiO₂ core/shell

- structure as light scattering material for highly efficient dye-sensitized solar cells.” *ACS Applied Materials & Interfaces*, vol. 5, no. 11, pp.4815–4820, Jun. 2013.
- [5]. Z. Wang, Q. Tang, B. He, H. Chen, and L. Yu. “Efficient dye-sensitized solar cells from curved silicate microsheet caged TiO₂ photoanodes. An avenue of enhancing light harvesting.” *Electrochimica Acta*, vol. 178, pp.18–24, 2015.
- [6]. N. Fadhilah, E. R. J. Alhadi, and D. D. Risanti. “Towards better light harvesting capability for DSSC (dye sensitized solar cells) through addition of Au@SiO₂ core-shell nanoparticles.” in *AIP Conf. Proc.*, vol. 1945, no. 1, 2018, p. 20029.
- [7]. F. A. F. Sugiono and D.D. Risanti. “Tunable surface plasmon resonances of Au@TiO₂ core-shell nanoparticles on the dssc (dye sensitized solar cells) performance.” *Jurnal Sains Materi Indonesia*, vol. 20, no. 3, pp.106-110, 2019.
- [8]. H. A. Budiarti, R. N. Puspitasari, A. M. Hatta, Sekartedjo, and D. D. Risanti. “Synthesis and characterization of TiO₂@SiO₂ and SiO₂@TiO₂ core-shell structure using lapindo mud extract via sol-gel method.” *Procedia Engineering*, vol. 170, pp.65–71, 2017.
- [9]. R. N. Puspitasari, H. A. Budiarti, A. M. Hatta, Sekartedjo, and D. D. Risanti. “Enhanced dye-sensitized solar cells performance through novel core-shell structure of gold nanoparticles and nano-silica extracted from lapindo mud vulcano.” *Procedia Engineering*, vol. 170, pp.93–100, 2017.
- [10]. N. Fadhilah, D. Y. Pratama, D. Sawitri, and D. D. Risanti. “Preparation of Au@TiO₂@SiO₂ core-shell nanostructure and their light harvesting capability on DSSC (dye sensitized solar cells).” in *AIP Conf. Proc.*, vol. 2088, no. 1, 2019, p. 60007.
- [11]. I. Paramudita and D. D. Risanti. “Sintesis dan Karakterisasi Au-SiO₂ menggunakan silica gel dengan variasi pH.” *Jurnal Sains Materi Indonesia*, vol. 19, no. 4, pp.174–178, 2018.
- [12]. I. Paramudita, N. Fadhilah, and D. D. Risanti. “Gold nanoparticles and silicate microsheet modified photoanode for dye sensitized solar cells.” *Materials Science Forum*, vol. 936, pp.77–81, 2018.
- [13]. M. A. K. L. Dissanayake, J. M. K. W. Kumari, G. K. R. Senadeera, and C. A. Thotawatthage. “Efficiency enhancement in plasmonic dye-sensitized solar cells with TiO₂ photoanodes incorporating gold and silver nanoparticles.” *Journal of Applied Electrochemistry*, vol. 46, no. 1, pp.47–58, 2016.
- [14]. H. Pujiarti, R. Hidayat, and P. Wulandari. “Enhanced efficiency in dye-sensitized solar cell by localized surface plasmon resonance effect of gold nanoparticles.” *Journal of Nonlinear Optical Physics & Materials*, vol. 28, no. 04, p. 1950040, Dec. 2019.
- [15]. A. Neshat and R. Safdari. “Enhancement in dye-sensitized solar cells using surface plasmon resonance effects from colloidal core-shell Au@SiO₂ nanoparticles.” *Chemistry Select*, vol. 4, no. 17, pp.4995–5001, May 2019.
- [16]. S. Supriyono, H. Surahman, Y. K. Krisnandi, and J. Gunlazuardi. “Photocurrent enhancement of CdS quantum dot sensitized TiO₂ electrode in the presence of gold nano particles.” *Jurnal Sains Materi Indonesia*, vol. 16, no. 3, pp.112–117, 2015.
- [17]. Y. H. Jang, Y. J. Jang, S. T. Kochuveedu, M. Byun, Z. Lin, and D. H. Kim. “Plasmonic dye-sensitized solar cells incorporated with Au–TiO₂ nanostructures with tailored configurations.” *Nanoscale*, vol. 6, no. 3, pp.1823–1832, 2014.
- [18]. S. W. Sheehan, H. Noh, G. W. Brudvig, H. Cao, and C. A. Schmittenmaer. “Plasmonic enhancement of dye-sensitized solar cells using core–shell–shell nanostructures.” *The Journal of Physical Chemistry C*, vol. 117, no. 2, pp.927–934, Jan. 2013.
- [19]. M. Li, M. Li, Y. Zhu, Y. Tang, L. Bai, W. Lei, Z. Wang, and X. Zhao. “Scattering and plasmonic synergetic enhancement of the performance of dye-sensitized solar cells by double-shell SiO₂@Au@TiO₂ microspheres.” *Nanotechnology*, vol. 28, no. 26, p. 265202, 2017.
- [20]. M. Li, N. Yuan, Y. Tang, L. Pei, Y. Zhu, J. Liu, L. Bai, and M. Li. “Performance optimization of dye-sensitized solar cells by gradient-ascent architecture of SiO₂@Au@TiO₂ microspheres embedded with Au nanoparticles.” *Journal of Materials Science & Technology*, vol. 35, no. 4, pp.604–609, 2019.
- [21]. L. Bai, J. Liu, Y. Tang, C. Wang, J. Wen, H. Wu, W. He, and R. Sun. “Synergistic enhancements in the performances of dye-sensitized solar cells by the scattering and plasmon resonance of Au-nanoparticle multi-shell hollow nanospheres.” *International Journal of Energy Research*, vol. 44, no. 8, pp.7026–7034, Jun. 2020.
- [22]. J. Waxenegger, A. Trügler, and U. Hohenester. “Plasmonics simulations with the MNPBEM

- toolbox: consideration of substrates and layer structures.” *Computer Physics Communications*, vol. 193, pp.138–150, 2015.
- [23]. S. L. Westcott, S. J. Oldenburg, T. R. Lee, and N. J. Halas. “Formation and adsorption of clusters of gold nanoparticles onto functionalized silica nanoparticle surfaces.” *Langmuir*, vol. 14, no. 19, pp.5396–5401, Sep. 1998.
- [24]. C. Dahmen, B. Schmidt, and G. von Plessen. “Radiation damping in metal nanoparticle pairs.” *Nano Letters*, vol. 7, no. 2, pp.318–322, Feb. 2007.
- [25]. T. K. Nguyen, K. Q. Le, A. Canimoglu, and N. Can. “Broadband luminescence of Cu nanoparticles fabricated in SiO₂ by ion implantation.” *Applied Radiation and Isotopes*, vol. 115, pp.109–112, 2016.
- [26]. U. Kreibig and M. Vollmer, *Optical Properties of Metal Clusters*. Berlin-Heidelberg: Springer Series in Materials Science Vol. 25, 1995.
- [27]. S.-J. Ha and J. H. Moon. “In-situ fabrication of macroporous films for dye-sensitized solar cells: formation of the scattering layer and the gelation of electrolytes.” *Scientific Reports*, vol. 4, no. 1, p. 5375, 2014.
- [28]. S. P. Lim, A. Pandikumar, N. M. Huang, and H. N. Lim. “Facile synthesis of Au@TiO₂ nanocomposite and its application as a photoanode in dye-sensitized solar cells.” *RSC Advances*, vol. 5, no. 55, pp.44398–44407, 2015.
- [29]. T. Bora, H. H. Kyaw, S. Sarkar, S. K. Pal, and J. Dutta. “Highly efficient ZnO/Au Schottky barrier dye-sensitized solar cells: Role of gold nanoparticles on the charge-transfer process” *Beilstein Journal of Nanotechnology*, vol. 2, pp.681–690, 2011.
- [30]. M. M. Byranvand, A. Dabirian, A. N. Kharat, and N. Taghavinia. “Photonic design of embedded dielectric scatterers for dye sensitized solar cells.” *RSC Advances*, vol. 5, no. 42, pp.33098–33104, 2015.

